Journal of Electronic Research and Application, 2026, Volume 10, Issue 3
http://ojs.bbwpublisher.com/index.php/JERA
ISSN Online: 2208-3510
ISSN Print: 2208-3502

Integrated Volt-Energy Storage-Lighting System for Smart Road Lighting Based on Distributed MPPT: A Review of Hardware Design and Economic Analysis

Xiangran Chen[1†], Jierui Feng[2†], Yuying Pan[3], Mingwei Li[4], Yanran Li[5], Yuhan Song[6]

[1]School of Economics and Management, Chongqing Jiaotong University, Chongqing, China
[2]School of Civil Engineering, Chongqing Jiaotong University, Chongqing, China
[3]College of Chongqing Jiaotong University, Chongqing, China
[4]School of Architecture and Planning, Chongqing Jiaotong University, Chongqing, China
[5]School of Economics and Management, Chongqing Jiaotong University, Chongqing, China
[6]Chongqing Jiaotong University School of Economics and Management, Chongqing, China
[†]These authors made equal contributions to this work.

Abstract: Smart street lights are the key carrier of smart cities and dual carbon goals. Aiming at the problems of high energy consumption of street lamps, extensive control, lack of dynamic adaptation capabilities of existing smart street lamps, and the vulnerability of centralized photovoltaics to shadows and module aging, this paper proposes a distributed MPPT photovoltaic-energy storage-lighting integrated system. The system hardware integrates high-precision sampling, STM32 main control, DC-DC conversion and lithium iron phosphate battery management; The software integrates traffic flow monitoring, people flow statistics and multi-factor linear regression dimming algorithm to realize perception and dynamic dimming. Through the three-layer architecture of perception-processing-cloud, the system not only improves the efficiency of photovoltaic power generation and adapts to complex lighting, but also has been preliminarily verified to have significant technical feasibility and economic value in terms of power generation efficiency, energy saving and cost reduction, and full life cycle costs.

Keywords: Distributed MPPT; Smart street lamps; Hardware design; Investment income analysis; Shadow inhomogeneity

Online publication: April 22, 2026

1 . Introduction

Under the guidance of the national strategic goal of "carbon peaking in 2030 and carbon neutrality in 2060", the construction of smart cities has put forward urgent requirements for the intelligence and energy saving of road lighting systems [1]. As a clean distributed energy source, the application of photovoltaic energy in street lighting scenarios has become an important trend. However, centralized photovoltaic power supply systems are easily affected by local shadows in complex cities, resulting in a sharp drop in overall power generation efficiency,

and widespread extensive control and unreasonable layout, problems such as high operation and maintenance costs. At present, my country's traffic street lamps have a large scale and significant energy-saving potential, but most of the research on smart street lamps is still in the initial stage, lacking an intelligent control system that integrates perception and human and vehicle flow, and fails to optimize energy utilization. In response to the above bottlenecks, this paper proposes a "photovoltaic-energy storage-lighting integration" smart street lighting system, which improves the power generation efficiency under shadow conditions through distributed MPPT technology, and combines intelligent control algorithms to achieve "on-demand lighting" [2]. At present, relevant research mostly focuses on algorithm simulation and conceptual design, and there are still obvious gaps in low-cost MPPT hardware circuits suitable for single lamps, multi-module integration adaptability, and quantitative analysis of full life cycle economic benefits in complex scenarios.

This paper will carry out research from four dimensions: theoretical basis, hardware design, economic benefits and conclusion outlook, explain the core technology of the system in turn, design the hardware circuit of the distributed MPPT controller in detail, build an economic benefit comparison model and conduct quantitative analysis, and finally summarize the technical advantages And look forward to the future direction, in order to provide support for the practical application and promotion of smart street lighting systems (**Figure 1**).

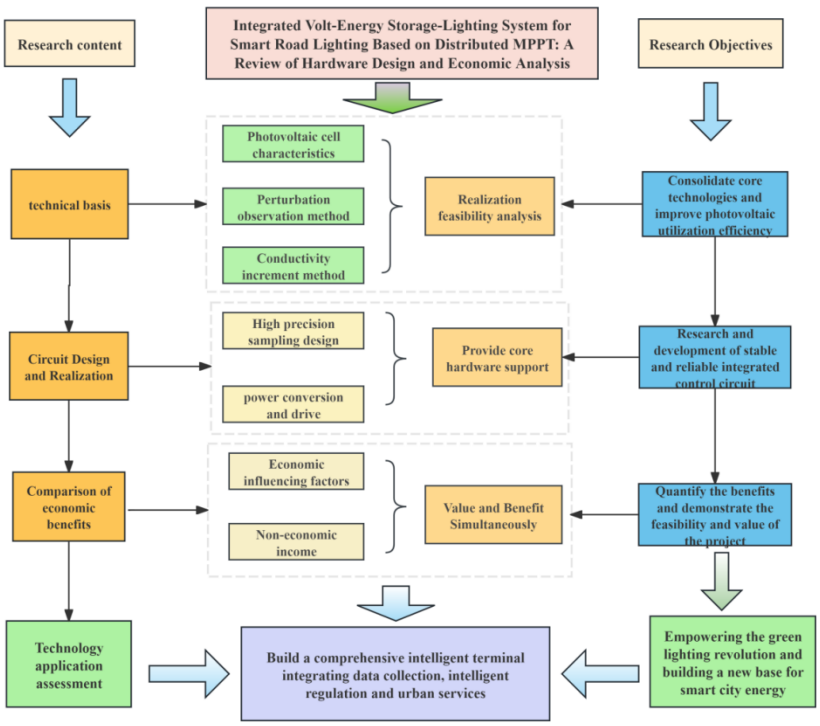

Figure 1. Full process flowchart.

2. Key technology basis of distributed MPPT system

2.1. Photovoltaic cell characteristics and maximum power point tracking principle

The output power of photovoltaic cells is significantly affected by factors such as irradiance, temperature and shadow, and its maximum power point (MPP) will drift dynamically with changes [3]. The higher the irradiance, the larger the corresponding power value of MPP, and the MPP will move along the power-voltage curve; The

increase in temperature will cause the open circuit voltage of the photovoltaic module to drop, make the MPP shift to the low voltage direction, and at the same time its power peak. In addition, the shadow may cause the "hot spot effect" of the photovoltaic module, resulting in multiple peaks in the output characteristic curve, making the MPP distribution scattered and unstable, and seriously affecting the overall output power of the system. Maximum power point tracking(MPPT) technology has become the key to improve the efficiency of photovoltaic utilization.

The basic working principle of MPPT is to collect the output voltage and current of the photovoltaic panel in real time through the sampling circuit, calculate the instantaneous output power, and judge the position deviation between the current working point and the real-time maximum power point according to the specific tracking algorithm, and determine the adjustment direction of the voltage or current [4]. After that, by controlling the duty cycle of the DC-DC power converter circuit, the equivalent load of the photovoltaic panel is changed, and the working voltage and current of the photovoltaic panel are dynamically adjusted, so that the working point of the system is close to and stable near the maximum power point. The closed-loop control can realize the state that the PV panel is still close to the maximum power output when the parameters change.

2.2. Mainstream MPPT algorithms and feasibility analysis of hardware implementation

2.2.1. Perturbation observation method

By changing the output voltage (or current) of the photovoltaic cell periodically, the disturbance observation method detects the power change trend, so that the disturbance direction gradually approaches the MPP [5]. This algorithm is simple in principle, does not need the accurate photovoltaic parameter model, the hardware sampling link is relatively simple, and the dynamic response is fast. It is the least difficult MPPT algorithm to implement on the microcontroller side [6]. Core steps such as voltage/current sampling, power calculation, comparison, and duty cycle adjustment can be completed only by relying on MCU general-purpose peripherals, and even 8-bit or 16-bit low-cost MCUs can be competent. The algorithm runs stably, does not have the problem of integral saturation or parameter drift, and occupies low resource. However, it also has some shortcomings, such as steady-state oscillation, tracking misjudgment when the irradiance changes rapidly, and the contradiction between the disturbance step size and the tracking performance. Its core parameters (disturbance step size and sampling interval) have clear requirements for hardware sampling. If the step size is too small, high-resolution ADC is required, and if it is too large, it will cause steady-state loss; If the sampling interval is too short, unstable transient values may be collected, resulting in power judgment errors, and if the sampling interval is too long, the speed will be tracked. For single-rod PV systems (whose PV array transient response time is generally 10–50ms), the sampling interval is usually set to 50-200ms. Considering the low-cost requirements, a disturbance step size of 1–3% can generally be used with a 10-bit ADC; The sampling interval is adapted to the transient response time of the system and is set to 50–200ms. Under this requirement, the universal ADC of low-cost MCU is fully sampled rate required.

2.2.2. Conductance increment method

The conductance increment method is based on the mathematical model of the P-U characteristics of the photovoltaic array [7]. Based on the theory of the differential of power to voltage at the MPP, the position of the operating point relative to the MPP is judged by calculating the relationship between the instantaneous conductance and the conductance increment. The algorithm has good steady-state performance, strong anti-

interference ability, and accurate dynamic tracking, but the principle is more complex, and the calculation amount is large, which requires high hardware sampling accuracy and MCU computing ability. It usually requires 12-bit and above high-resolution ADCs, low-drift voltage/current sensors, and precision signal conditioning circuits, and relies on 32-bit high-performance MCUs to perform floating-point operations [8]. At the same time, the algorithm has strict requirements on sampling rate and synchronization control, resulting in significant hardware cost and system design complexity, which is difficult to match the application requirements of low-cost, single-pole photovoltaic systems.

2.2.3. Other algorithms

Intelligent MPPT algorithms such as fuzzy control, particle swarm optimization, and neural networks, although they can effectively deal with the tracking problems of the algorithm under complex conditions, and have the advantages of strong anti-interference ability, good global optimization ability, and fast tracking speed, they are common [9–11]. There are problems such as high computing complexity, strict hardware requirements, and difficult debugging. These algorithms usually rely on high-performance MCU or even DSP support, and the hardware cost can reach 5–10 times that of the disturbance observation method. It is an excess performance and low applicability in low-cost single-rod photovoltaic systems with conventional illumination [12]. On the other hand, although the hardware implementation of simple algorithms such as the constant voltage method is simpler, they cannot adapt to the changes of irradiance and temperature, and the tracking accuracy is very low [13]. They are only suitable for ultra-low-cost simple systems, and it is difficult to meet the power output requirements of conventional photovoltaic systems.

To sum up, the perturbation-observation method and its variants are the preferred algorithms for low-cost, single-pole photovoltaic systems in hardware implementation. The main reason is that the algorithm has the lowest implementation cost, only 8-bit/16-bit general-purpose MCU, 10-bit ADC and basic voltage/current sampling link are required, no additional expensive hardware is required, and the algorithm implementation and debugging are relatively simple, the code volume is small, and the logic is clear, even entry-level embedded personnel can get started quickly, suitable for low-cost design requirements of rapid mass production [14]. The steady-state oscillation problem existing in its version can be effectively optimized through improved algorithms such as variable step size and hysteresis disturbance, so that the steady-state oscillation loss is reduced to less than 1%, and at the same time, the dynamic response speed is good. Power utilization target.

2.3. Selection of energy storage technology

As an energy storage unit, the new high-cycle lithium iron phosphate battery performs outstandingly in outdoor work: its charge and discharge cycles can reach 2,000times (remaining capacity rate > 80%) [15]. Excellent thermal stability, decomposition temperature above 200 ℃, not easy to catch fire or short circuit in the case of overcharge, overdischarge or short circuit; The voltage platform is stable (the voltage in the mid-discharge period is maintained at 3.0V–3.2V), and the output power is stable; It supports 0.2C–1C conventional charging and discharging, has no memory effect, can be charged at any time, and can work stably in a wide temperature range of -20°C to 60°C. These characteristics make it highly suitable for the working conditions of street lamps in harsh outdoor conditions.

The system adopts a “constant current-constant voltage” charging management strategy: in the charging stage, it first charges at a constant current of 0.3C to 3.65V, and then switches to constant voltage charging

until the current drops to 0.05C, so as to avoid overcharging and damage to the battery [16]. In the discharge stage, a hierarchical discharge strategy is adopted. Combined with the energy consumption demand of street lamps (the working current of 60W LED lamps is about 5A), 20% of the remaining power is set as the lower discharge limit. The system supports dual power supply access of mains power and solar energy at the same time, ensuring that the basic lighting can be maintained for no less than 8 hours after the mains power is cut off. The charging and discharging management strategy can realize closed-loop control through the timer and ADC sampling of STM32 single-chip microcomputer, which is conducive to prolonging the battery life and operation and maintenance costs.

3. Design and implementation of hardware circuit for distributed MPPT controller

3.1. Overall hardware architecture of the system

The system adopts an independent single-pole power supply structure. Its core energy management and transmission path is: the DC energy output by the photovoltaic panel is first optimized by the MPPT charging controller, and then charged for the lithium iron phosphate battery energy storage unit. As the energy center of the system, the energy storage unit provides a stable power supply for subsequent LED drives and lighting loads, as well as various intelligent perception and control modules [17]. As the core of the power supply system, MPPT controller integrates key sub-modules such as high-precision sampling circuit, MCU main control unit, DC-DC power conversion circuit, battery management and protection circuit, and communication interface. These modules work together to realize the maximum power point tracking of photovoltaic electric energy, high-efficiency electric energy conversion, intelligent charging and discharging management and safety protection of lithium batteries, and communicate and interact with the upper system, so as to provide the stability, efficiency and autonomy of the whole street lamp system. Operation provides core hardware support.

3.2. High-precision sampling circuit design

3.2.1. Voltage sampling circuit

Voltage sampling objects include photovoltaic terminal voltage (12V–24V) and battery terminal voltage (10.8V–13.6V) [18]. The design uses a precision resistor voltage dividing network (ratio 10:1) to reduce the voltage. In order to reduce the influence of temperature drift, the precision metal film resistor with an error of ± 0.1% is selected for the voltage dividing resistor. The signal after voltage division is filtered out of high-frequency noise by an RC filter circuit ($R = 10k\Omega$, $C = 0.1\mu F$), and then buffered and impedance matched by a voltage follower composed of an LM324 operational amplifier to ensure that the input signal of the ADC channel of the STM32 single-chip microcomputer is stable and reliable. In order to further improve the sampling accuracy, the reference voltage of the ADC adopts the high-precision reference source REF3030 (error ± 0.1%), and the final voltage sampling accuracy is better than ± 0.5%.

3.2.2. Analysis and selection of current sampling schemes

The accuracy and stability of current sampling directly determine the tracking performance of the disturbance-observation MPPT algorithm. In order to achieve low-cost and high-reliability system design, it is necessary to comprehensively compare the mainstream current sampling schemes. This design finally chooses the “sampling resistor high common mode rejection ratio (CMRR) operational amplifier” scheme instead of Hall current sensor, mainly based on the following four dimensions:

(1) Accuracy and linearity: The perturbation observation method needs to accurately identify small power changes (usually to distinguish ≥ ± 0.5% differences) to avoid tracking misjudgments. The sampling resistor scheme has excellent linearity (full range ≤ ± 0.1%), especially in low light and low current (< 5A) scenarios, with high CMRR (≥ 80dB) operational amplifiers, it can effectively suppress common-mode interference, accurately capture power changes, and prevent The algorithm oscillates near the maximum power point (MPP). In contrast, Hall sensors (especially open-loop sensors) have poor linearity (± 1%~ ± 3%), and nonlinear and noise problems are more prominent when the current is small, which can easily lead to power calculation deviations and algorithm misjudgments, resulting in additional power generation losses;

(2) Cost control: Follow the design goal of "low cost and easy implementation" of the project. The cost advantage of the sampling resistor solution is significant: the unit price of precision sampling resistor and high CMRR operational amplifier is low, and there is no need for peripheral isolation or magnetic core, and the circuit is simple. Hall sensors (especially closed-loop sensors) have a high unit price, and may require additional power supply and shielding design, which reduces the complexity and overall cost of the system, and is not conducive to the large-scale promotion of the solution;

(3) Temperature stability: The operating temperature range of street lamps is wide (-20°C~60°C) [19]. The sampling resistance scheme can control the sampling error in the whole temperature range within ± 0.3% by selecting low temperature coefficient components (such as metal foil resistance ≤ 5ppm/℃, operational amplifier temperature drift ≤ 0.1μV/℃) combined with software compensation algorithm, ensuring the stability of the algorithm. The Hall sensor is greatly affected by the temperature, and its magnetic core is prone to significant drift to the temperature at extreme temperatures, which affects the sampling accuracy and may cause the MPP tracking point to shift;

(4) Bandwidth and dynamic response: For the typical parameters set by the perturbation observation method (disturbance step size 0.1V, sampling interval 0.5s), the required sampling bandwidth is about 1kHz~10kHz. The sampling resistor scheme cooperates with operational amplifier (bandwidth is usually 1MHz~10MHz) and appropriate RC filtering (cut-off is about 159Hz), has a fast response speed (time constant is about 1ms), and can track current changes in real time. Although the bandwidth of the Hall sensor may be higher, the high-frequency noise is large. Strengthening the filtering to suppress the noise will introduce signal delay (≥ 5ms), which may affect the timely response of the algorithm to sudden illumination changes.

To sum up, the "sampling resistance high CMRR operational amplifier" solution is more in line with the design requirements of this distributed MPPT controller in terms of accuracy, cost, temperature drift and dynamic response, and is the choice to achieve high-performance and low-cost MPPT tracking.

3.2.3. Temperature sampling circuit

The integrated DHT11 temperature and humidity sensor is selected for temperature sampling [20]. Its temperature measurement range is 0°C to 50°C, and the accuracy is ±2°C. It communicates with the STM32 single-chip microcomputer through the I2C interface, and the sampling interval is set to 1 second. The collected temperature data serves two core functions: one is to provide temperature compensation parameters for the MPPT algorithm, and correct the change of photovoltaic cell MPP with temperature; The second is to connect to the battery management system (BMS). When the temperature exceeds the safe range (such as lower than

0°C or higher than 50°C), the charging and discharging current will be automatically or cut off to ensure battery safety.

3.3. Power conversion and drive circuit design

Buck DC-DC converter is selected as the core power conversion topology. The selection is based on the actual voltage matching relationship of the system: the operating voltage of the photovoltaic terminal (usually 18V~24V, the lowest is 12V) is higher than the voltage range of the battery terminal (10.8V~13.6V) in most working conditions. Even under extreme crossover conditions (photovoltaic minimum 12Vvs. cell 13.6V), the voltages of the two are basically the same, and the Buck topology can still operate in critical or extremely small duty cycle states. Therefore, there is no need to adopt a more complex and costly Buck-Boost Buck-Boost topology. With its advantages of simple structure, few power devices, high conversion efficiency, and low cost, the Buck topology fully meets the design requirements of a single-pole photovoltaic street lamp system.

The power switching device is N-channel enhanced power MOSFET. In low-power, low-voltage street lamp application scenarios, MOSFETs have the advantages of lower switching losses and simpler drive circuits than IGBTs. The drive circuit adopts a discrete device push-pull scheme with low cost and high efficiency. The circuit is composed of S8050 (NPN type) and S8550 (PNP type) transistors, which can provide fast gate charge and discharge capabilities and ensure fast switching of MOSFET. Gate series resistors (10~100Ω) are used to balance switching speed and electromagnetic interference (EMI). The 3.3V or 5V PWM signal generated by the MCU can directly drive this push-pull circuit.

4. Comparative evaluation of economic benefits between distributed and centralized solutions

4.1. Core definition and architecture differences

The centralized solution adopts the architecture of "central control platform unified transmission network". All street lamp terminals (including sensors, LED light sources and controllers) are wired (such as optical fiber/cable) or wirelessly connected to a single central platform, which centrally completes data processing and command issuance. Its hardware is highly dependent on central servers and large-scale cabling systems (such as fiber optic solutions). The distributed solution adopts a hierarchical architecture of "regional local autonomous control". The system deploys multiple areas according to geographical areas, and the street lamp terminals in each area are first connected to the local area to realize data preprocessing and real-time control (such as dimming and fault warning); The area then interacts with the cloud platform through wireless such as 5G/LoRaWAN. Its hardware is centered on modular area and wireless communication devices (such as layers in intelligent networking solutions) [21].

4.2. Analysis of key economic factors

4.2.1. Component prices

The cost of centralized components accounts for about 40–50% of the total initial investment. If the component price drops by 10%, it can only drive the total investment by 4–5%, because core costs such as central servers and large-scale wiring account for a high proportion and are not affected by component prices. The cost of distributed components accounts for 60–70% of the total initial investment (area and terminal sensors account for a relatively high proportion). A 10% drop in component prices can result in a total investment of 6–7%.

Based on a project of 100,000 street lamps, the upfront cost can be saved by 150,000 to 200,000 yuan. The decrease in module prices is more significant for improving the economy of distributed solutions, especially in photovoltaic integration projects (the decrease in the price of photovoltaic panels can directly affect the cost of distributed energy storage systems) [22].

4.2.2. Controller costs

Centrally rely on a central controller with high computing power (the cost is about 50,000–100,000 yuan per unit). Every 10% reduction in its cost can make the total initial investment 3–5% (the proportion of central equipment is high). Distributed relies on a large number of low-cost local controllers (the cost is about 50–100 yuan per unit). For every 10% reduction in its cost, the impact on the total initial investment is only 1–2% (the impact is small after the cost is allocated by the region). The cost reduction of the controller is more critical to improve the economy of the centralized scheme. However, the initial cost base of centralized controllers is large. Even after the cost decreases, its total control cost (about 80,000 yuan for 100,000 projects) is usually still higher than that of distributed solutions (about 60,000 yuan).

4.2.3. Regional sunshine and shadow conditions

The economic difference between the two schemes is small in the area with sufficient sunshine. Centralized solutions can optimize charging through unified scheduling, but distributed solutions usually have 5–8% higher charging efficiency by virtue of local fast adaptation capabilities (charging strategies within 100ms after sudden sunshine changes). In areas with dense shadows, the unified charging strategy of the centralized solution cannot adapt to local shadows, which may lead to insufficient charging in shadowed areas and the need to rely on the grid for power replenishment and electricity expenses. Distributed areas can identify shadows in real time, and dynamic single-light charging power (such as extending charging time for shadow areas, giving priority to power storage in non-shadow areas), resulting in dependence on the power grid, making the cost of energy storage systems 15–20%. In densely shaded areas, the economic advantages of distributed solutions are more prominent. In areas with sufficient sunshine, although the economic difference between the two has narrowed, the distributed solution still has the comprehensive advantage of lower operation and maintenance costs.

4.3. Non-economic gains

Distributed solutions show significant systemic advantages at the non-economic level. In terms of reliability, its “regional autonomy” architecture strictly limits the scope of failure to local areas (usually 50-100 lights), and combined with the multi-link redundant backup mechanism, the overall availability of the system is greatly improved from about 95% of the centralized solution to more than 99.9%, effectively avoiding the inherent risk of “single point of failure, paralysis of the entire network” of the centralized architecture [23]. In terms of flexibility and scalability, the modular design of the distributed solution supports “plug and play”, which makes the expansion cost of new functions or devices about 70%, shortens the deployment cycle from several months to several weeks, and can respond agilely Diversified and dynamically changing urban needs. Most importantly, in terms of asset health management, the distributed architecture relies on the real-time monitoring and precise control of the status of the single-lamp energy storage battery realized by the region, which can reduce the average annual decay rate of the battery from about 15% under the centralized unified strategy to less than 8%, thereby extending the expected service life of the battery from 3–4 years to 5–6 years [24]. This not only greatly increases the cost of battery replacement and operation and maintenance, but also reflects its deep advantages in

improving system availability and full life cycle value [25].

5. Conclusion

The distributed MPPT hardware controller realizes the independent high-precision maximum power point tracking (MPPT) of each photovoltaic panel by adopting the sampling architecture of "precision voltage division filter conditioning high-precision benchmark", the improved adaptive tracking algorithm based on the disturbance observation method, and the wide voltage dynamic management strategy for lithium iron phosphate batteries. Its sampling comprehensive error is controlled within ± 0. 5%, and the tracking efficiency exceeds 95%, thus effectively solving the problems of uneven illumination and shadow occlusion caused by high-rise buildings and trees in the city. The power generation efficiency of a single photovoltaic panel can be increased by 15–20%. Although the initial hardware cost of this solution is slightly increased, with the significant power generation gain and system redundancy reliability, it can cover the cost and create additional energy saving benefits throughout the product life cycle. In the future, the technology will evolve in the direction of high hardware integration and low power consumption, algorithm adaptive prediction, and system IoT node, through the introduction of dedicated chips, intelligent power modules, predictive models and reinforcement learning, and deep integration with smart city platforms. Finally, it will be upgraded from a single lighting controller to a comprehensive intelligent terminal integrating data acquisition, intelligent regulation and urban services.

Disclosure statement

The authors declare no conflict of interest.

References

[1] Krishna V, et al., 2026, Editorial Article (Special Issue): Measurement, Control and Security of Systems for Smart Cities. Measurement: Sensors, 2026(44): 101990.

[2] Değermenci M, Yalman Y, Olcay K, 2026, MPPT Algorithms for Grid-Connected Solar Systems including Deep Learning Approaches. Scientific Reports.

[3] Lal M, et al., 2026, Photogalvanics for Solar Energy Conversion and Storage: A Review on Progress of PG Cells. Next Research, 2026(5): 101331.

[4] Refaat O, et al., 2026, Potentials of Upcycling Photovoltaic Panels Waste in Construction: A Comparative Review. Developments in the Built Environment, 2026(25): 100845.

[5] Ni H, et al., 2025, Enhancing Robustness in Photoacoustic Detection of Dissolved Acetylene in Transformer Oil: Temperature Effects on Resonance Frequency and Suppression Using the Perturbation Observation Method. Energies, 18(24): 6512.

[6] Hajar A, Ahmed G, Benachir E, Innovative Neural Network and Fuzzy Logic Control Techniques for Single-Phase Grid-Connected Photovoltaic Systems using Dual-Core DSP Microcontroller in Smart Home Applications. Measurement and Control, 59(2): 232–244.

[7] Andrasto T, et al., 2024, Incremental Conductance Method in Maximum Power Point Tracking. IOP Conference Series: Earth and Environmental Science, 1381(1): 012023.

[8] Maghraby A, Ahmed H, Abougindia I, 2025, An Ultra-Low Noise Dynamic Comparator for Low-Power, High-

Resolution SAR ADCs. Circuits, Systems, and Signal Processing, 2025(prepublish): 1–15.

[9] Leite D, et al., 2026, Evolving Granular Fuzzy Control: Overview, Case Study on the Chaotic Hénon Map, and Research Outlook. Applied Soft Computing, 2026(190): 114639.

[10] Li H, et al., 2026, Impedance Force Control for Industrial Robot based on Unified Residual Compensation Iterative Learning Control and Multi-Directional Particle Swarm Optimization, Proceedings of the Institution of Mechanical Engineers, Part C: Journal of Mechanical Engineering Science, 240(4): 1214–1228.

[11] Abdelrahman N, Uth S, 2026, Data-Efficient Prediction in Tableting using Word Embeddings and Empirically-Guided Neural Networks. International Journal of Pharmaceutics: X, 2026(11): 100458.

[12] David J, Volling T, 2026, Multi-Objective Ergonomic–Economic Project Scheduling in Construction: The Case of Photovoltaic System Installation. Computers & Industrial Engineering, 2026(213): 111828.

[13] Dita R, et al., 2025, Development of a Buck Converter for Efficient Energy Storage Integration Using Constant Voltage (CV) Methods. Energy Engineering, 122(6): 2355–2370.

[14] Oleschuk V, 2025, Synchronization and Symmetrization of Base Voltages of Electronic Transformer-Based Converters in the Overmodulation Zone of Voltage Source Inverters. Surface Engineering and Applied Electrochemistry, 61(6): 951–959.

[15] Ling H, et al., 2026, Realizing Rapid Energy Storage and Efficient Release in a Tesla Valve Integrated Cold Energy Storage Unit for Data Center Cooling. Applied Thermal Engineering, 289(P1): 129683.

[16] Subashini M, Sumathi V, 2026, Adaptive Charging Strategies for Electric Vehicles: A Reinforcement Learning Approach to Demand Response and Resource Management. Energy Reports, 2026(15): 109015.

[17] Ghana Achieves Stable Power Supply, Eyes Green Future after Major Energy Reforms, 2025, M2 Presswire.

[18] Li J, et al., 2026, Novel Control Strategy for Voltage Control System Integrated with Photovoltaic System using Terminal Reaching Law-based Fast Integral Terminal Sliding Mode Concept. Electric Power Systems Research, 2026(253): 112548.

[19] Kong X, et al., 2026, Local Structural Engineering for Simultaneous Enhancement of Piezoelectricity and Temperature Stability in BiScO3-PbTiO3 Piezoceramics. Journal of Materials Science & Technology, 2026(268): 51–60.

[20] Lu J, et al., 2026, Multi-Physics Coupled Simulation and Hybrid Mechanistic Data Driven Modeling for High-Accuracy Radiation Error Correction in Sounding Temperature Sensors. Sensor Review, 46(2): 299–310.

[21] Bala I, Singh G, Tripathi S, Sustainable Technologies and Devices for Next-Generation Wireless Communication: CRC Press.

[22] Li L, Dai C, 2024, Internal and External Factors Influencing Rural Households' Investment Intentions in Building Photovoltaic Integration Projects. Energies, 17(5).

[23] De Deken J, Luigjes C, 2025, Federal Solidarity, Regional Autonomy and Institutional Moral Hazard. The Case of Belgian Unemployment Insurance and Activation Policies. Journal of European Social Policy, 35(5): 423–438.

[24] Alfahdi K, Gultekin H, Summad E, 2025, A Novel Global Health Index Framework for Asset Prognostics and Health Management in the Oil and Gas Industry. Scientific Reports.

[25] Li H, et al., 2013, Design on Distributed Reconfigurable Satellite Full Life Cycle Value Assessment System. Applied Mechanics and Materials, 482(482-482): 287–291.